International Journal of Modern Physics: Conference Series

JLAB12 AND THE STRUCTURE OF HADRON

M. CONTALBRIGO
INFN, Via Saragat 1 - blocco C
Ferrara, 44100, Italy
contalbrigo@fe.infn.it

Received Day Month Year
Revised Day Month Year

The investigation of the partonic degrees of freedom beyond collinear approximation (3D description) has been gained increasing interest in the last decade. The Thomas Jefferson National Laboratory, after the CEBAF upgrade to 12 GeV, will become the most complete facility for the investigation of the hadron structure in the valence region by scattering of polarized electron off various polarized nucleon targets. A compendium of the planned experiments is here presented.

Keywords: Structure of Hadrons, Spin, TMDs, GPDs, SIDIS, Hard Reactions

PACS numbers: 13.60.-r, 13.85.Ni, 13.87.Fh, 13.88.+e

1. The 3D Structure of Nucleons

Since decades, few questions challenge the interpretation of hadron structure and phenomena in Hadronic Physics in terms of perturbative QCD. Among the most intriguing, there is the spin budget of the nucleon, where there are missing contributions not quantified yet, and the surprising single-spin asymmetries, which do not vanish as expected with increasing energy. The questions above relate to one of the fundamental degree of freedom of the elementary particles, the spin, and its correlation with the particle motion (transverse momentum) of the partons.

Most of our present understanding of the internal structure of nucleons derives from inclusive deep-inelastic-scattering (DIS) experiments performed over the past four decades in different kinematic regimes at fixed-target experiments and collider machines. Based on the large amount of precise data provided by these experiments we have reached a good knowledge of the parton longitudinal-momentum and longitudinal-spin distributions of quarks in the nucleon, where "longitudinal" refers to the direction parallel to that of the exchanged virtual boson (the hard probe). In the recent years, new parton distributions have been introduced to describe the rich complexity of the hadron structure, taking into account the parton transverse degrees of freedom and moving toward the achievement of a 3D comprehension of the parton dynamics. At the same time new channels of investigation have been gained importance as the study of semi-inclusive and hard exclusive reactions.

This work presents a selection of the experiments planned at the JLab accelerator facility to address the mysteries of the hadron structure from a modern point of view.

2. Semi-inclusive Physics

A complete collinear description of the nucleon structure at leading order in an expansion in M/Q (twist expansion), where Q is the photon virtuality and M the nucleon mass, requires the knowledge of three fundamental parton distributions (PDFs): the momentum distribution $f_1(x)$, the helicity distribution $g_1(x)$, and the presently poorly known transversity distribution $h_1(x)$. Here x denotes the longitudinal momentum fraction carried by the partons and the scale dependence (on Q^2) has been neglected for simplicity. The transversity distribution reflects the quark transverse polarization in a transversely polarized nucleon and is related to the tensor charge of the nucleon [1]. Transversity has long remained unmeasured due to its chiral-odd nature, which prevents its measurement in inclusive deep-inelastic scattering: the transversity distribution can only be measured in conjunction with another chiral-odd object. One possibility is represented by semi-inclusive deep-inelastic scattering (SIDIS), where at least one final state hadron is detected in coincidence with the scattered lepton, which can be described in terms of convolutions of parton distribution and fragmentation functions.

Besides allowing to access transversity, SIDIS experiments open the way to the extraction of transverse-momentum-dependent (TMD) PDFs [2], which are increasingly gaining theoretical and experimental interest. Describing correlations between the quark or the nucleon polarization and the quark transverse momentum, i.e. spin-orbit correlations, the TMD distribution functions encode information on the 3-dimensional parton dynamics. There are eight independent leading-twist quark TMDs, ordered as a function of the nucleon N and quark q polarization in the following table:

N/q	Unpolarized	Longitudinal	Transverse
Unpolarized	f_1		$h_1^\perp$
Longitudinal		g_1	$h_{1L}^\perp$
Transverse	$f_{1T}^\perp$	g_{1T}	h_1, $h_{1T}^\perp$

The diagonal elements are the momentum, longitudinal and transverse spin distributions of partons above introduced. Off-diagonal elements require non-zero orbital angular momentum as they are related to the wave function overlap of Fock states of the nucleon with different angular momentum. The chiral-even distributions $f_{1T}^\perp$ and g_{1T} are the imaginary parts and the chiral-odd $h_1^\perp$ and $h_{1L}^\perp$ are the real parts of the interference terms between S and P wave components. The chiral-odd $h_{1T}^\perp$ function is sensitive to the D-wave component. The TMDs $f_{1T}^\perp$ and $h_1^\perp$ are known as the Sivers [3] and Boer-Mulders [4] functions. They require a non-trivial gauge link and therefore exhibit a peculiar process dependence: a sign change is expected moving from SIDIS to Drell-Yan processes. They describe unpolarized quarks in the transversely polarized nucleon and transversely polarized quarks in the unpolarized nucleon, respectively. The most simple mechanism that can lead to a Sivers (Boer-Mulders) function is a correlation between the spin of the nucleon (quarks) and the quark orbital angular momentum. In combination with a final state interaction that is on average attractive, such correlations manifest as azimuthal asymmetries of the produced hadron distribution.

TMDs can be accessed in SIDIS being associated with specific azimuthal angle dependencies of the cross-section, namely the dependence on combinations of the azimuthal angle of the target polarization ϕ_S and of the produced particle ϕ, both referred to the lepton scattering plane.

3. Hard Exclusive Physics

Generalized Parton Distributions (GPDs) [5], provide a multidimensional picture of the nucleon which is complementary to TMDs, correlating the longitudinal momentum fraction of partons with their transverse distance from the nucleon's center. For a spin-1/2 target, there are four leading twist GPDs, the vector GPDs H, E and the axial GPDs $\tilde{H}$, $\tilde{E}$, which describe elastic form factors and collinear parton distributions as kinematic limits. Having access to such a 3-dimensional image of the nucleon opens up new insights into the complex structure and dynamics of the nucleon. For example, certain moments of vector GPDs carry information on the elusive quark orbital angular momentum [6]. GPDs are accessible through exclusive processes that leave the target nucleon intact.

In addition to the constraints derived from the nucleon form factor and collinear PDF, Deeply virtual Compton scattering (DVCS) and Deeply virtual exclusive meson production (DVMP) are most suitable for mapping out the twist-2 GPDs as a function of the relevant kinematic variables x, Q^2, ξ and t, where ξ is the longitudinal momentum transfer to the quark, and t the transverse momentum transfer to the nucleon.

DVCS signals are one of the theoretically cleanest ways to access GPDs. They are small in the JLab kinematics but can be revealed through the interference with the calculable electromagnetic Bethe-Heitler (BH) process because of the identical initial and final states. The individual terms of the cross section can be decomposed into Furier harmonics in the azimuthal angle ϕ, which is defined as an angle between the lepton scattering plane and the photon production plane, and are expressed as different combinations of the so-called Compton Form Factors, which are convolutions of hard scattering coefficient functions with corresponding GPDs.

Deeply virtual exclusive meson production (pseudo scalar mesons and vector mesons) could play an important role in disentangling the flavor- and spin-dependence of GPDs. For exclusive mesons only the longitudinal photon coupling enables direct access to GPDs through the handbag mechanism and must be isolated from the transverse coupling. In addition, the dominance of the handbag mechanism

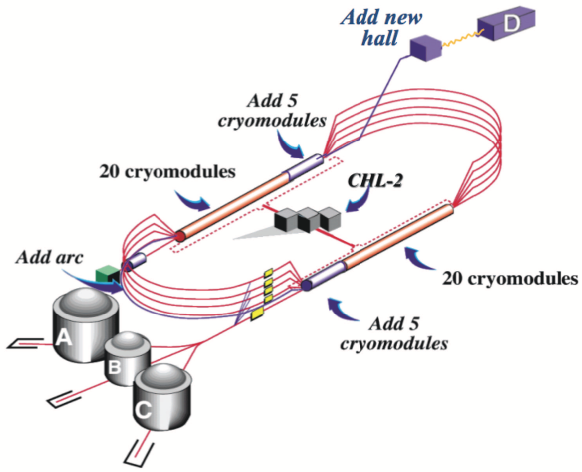

Fig. 1. The Jefferson Lab continuous electron beam accelerator facility with highlighted the components needed for the 12 GeV upgrade.

in the longitudinal cross section must first be established at the 12 GeV upgrade energy before meson production may be safely incorporated in a global fit of all hadronic reactions to extract GPDs.

4. The Thomas Jefferson National Laboratory

The continuous electron beam accelerator facility (CEBAF) of the Thomas Jefferson National Laboratory (JLab) is shown schematically in Fig.1. The two linear accelerators are based on superconducting RF technology. Spin polarized electrons have been accelerated by several passes in the linacs up to the final energy of 6 GeV during several years of successfully physics runs until the shut-down in May 2012 planned for the upgrade of the machine.

Several interesting results related to the spin structure of the nucleon have been achieved during the almost 15 years of CEBAF activity at 6 GeV. Among those are the evidence that the electric and magnetic moments of the proton does not scale as suggested by the historical Rosembluth separation [7] (likely because of underestimated radiative corrections), one of the first observations of a non-zero DVCS asymmetry [8], the hint of a different transverse momentum distribution for up and down quarks [9], the first TMD measurements with a transversely polarized ^{3}He target accessing the neutron distribution functions [10].

During the ongoing upgrade, five additional accelerating cryo-modules with four times higher gradients per unit length have been added to both linacs to reach a maximum energy of 11 GeV. One arc and one more path through the north linac have been added to accelerate the beam to 12 GeV and transport it to the new Hall

D. The Hall D focus, being on the study of hybrid mesons with exotic quantum numbers, goes beyond the scope of this paper and is not further discussed in the following. The base equipment in the historical Hall A, B and C is under upgrade or construction and is scheduled for completion in the next three years, following a complicated beam and spectrometer joined commissioning plan. The first low-momentum beam is expected in Hall A in the first half of 2014.

The 3D studies of the spin nucleon structure (in terms of TMDs and GPDs) will greatly benefit from the higher energy and luminosity available at 12 GeV. The main focus will be on the measurement of SIDIS processes and hard exclusive reactions in the full multi-dimensional phase space available thanks to the high luminosity reachable by the new machine. The precision mapping in multi-dimension will not only allow for the extraction of the new distributions, but also for a careful study of the reaction mechanism and related issues, such as the factorization, the separation/mixing in current-target fragmentation processes and the higher-twist effects.

The upgraded beam energy is ideal to efficiently map the quark valence region in the few GeV^2 hard-scale regime, covering a poorly explored region at large x which is crucial for the understanding of the spin dependent processes. A comprehensive program is in preparation to exploit the complementary of the different JLab experimental halls in the study the new quark distribution functions, as described in the following.

5. Hall C and the factorization tests

The 12 GeV SIDIS program in Hall C is focused on precision cross section measurements with the anticipated excellent systematic understanding of the HMS-SHMS high-momentum magnetic spectrometer pair. The well-shielded detector systems, the rigid connection to a sturdy pivot, the well-reproducible magnetic properties, and the access to the highest-luminosity data taking makes the HMS-SHMS setup optimal for a program of longitudinal to transverse cross-section separation and ratios of charged-meson cross sections.

Although the longitudinal to transverse cross-section ratio $R = \sigma_L/\sigma_T$ appears in the denominator of all the spin asymmetries related to the TMDs investigation, it is up to date unknown. The phenomenological analyses have typically assumed either zero or the values determined from inclusive DIS. The R value will likely have a pronounced dependence on the z value of the measured hadron, towards the exclusive limit. The precise measurement of the ratio R for charged pions and kaons [11], and neutral pions, will help to shed light on the nature of the reaction mechanism, in particular regarding the higher-twists contributions, which could be particularly important at the rather modest energies of JLab.

Precise measurements of the SIDIS cross sections for charged pions and kaons at low transverse momentum p_T from hydrogen and deuterium targets will provide, in combination with other data, a strong test of the theoretical understanding of SIDIS

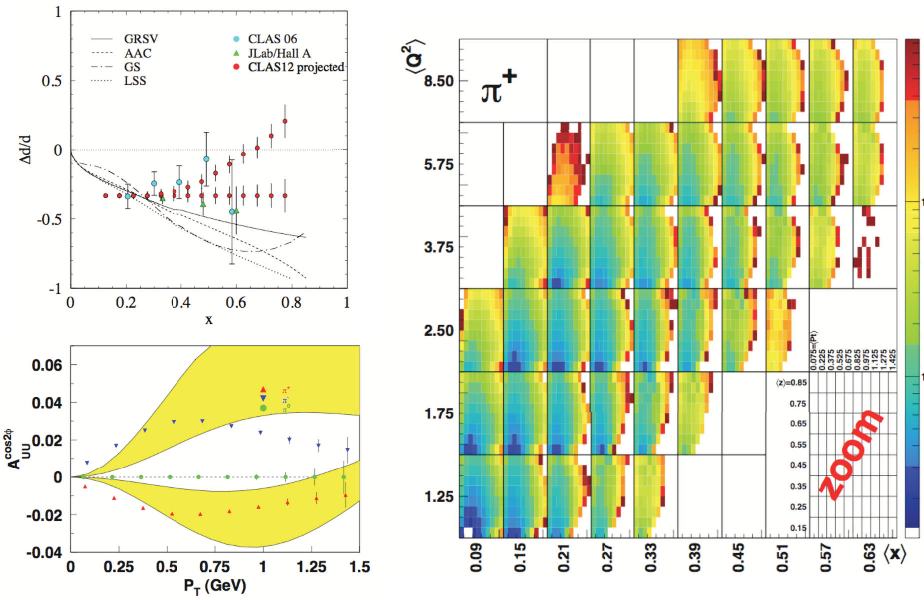

Fig. 2. Examples of TMDs measurements planned at 12 GeV. Top-Left: Expected results for $(\Delta d + \Delta\bar{d})/(d + \bar{d})$ helicity distribution [17]. The central values of the data are following two arbitrary curves to mimic the two categories of predictions (namely $\Delta d/d$ stays negative or tends to 1). Bottom-left: Expected statistical precision on the Boer-Mulders asymmetry [15] for pions as a function of p_T for $Q^2 > 2$ GeV^2. The yellow band between the two curves indicates the range of two model predictions. Right: Kinematic coverage of the 4-dimensional π^+ yield in Q^2, x, z, and p_T. The color code shows the projected uncertainties in each bin [20].

in terms of factorized parton distributions convoluted with fragmentation functions. In addition, they can be used in order to extract measures of the mean transverse momentum of up and down quarks in the nucleon [12]. The magnetic spectrometer setup will have by necessity a limited ability to constrain azimuthal moments of the SIDIS cross-sections, and analysis will often need to be complemented with that of the large-acceptance setups in other halls.

As a test of the GPD factorization, precise measurements are planned of the Q^2 dependence of the longitudinal component of the cross-section in exclusive pion [13] and kaon [14] electroproduction.

6. Hall B and the comprehensive exploration

Hall B with its wide kinematical coverage will provide a complete set of measurements extending from target to current fragmentation and to exclusive processes, using both unpolarized and polarized hydrogen and deuteron targets.

The large acceptance, and wide ranges in Q^2 and p_T, would allow to separate contributions from leading and sub-leading effects, extract the transverse momentum dependence of different TMDs, and study all relevant 3D partonic distributions

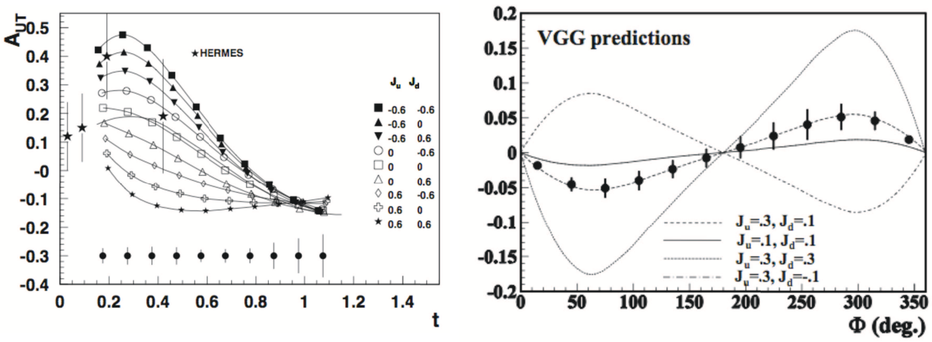

Fig. 3. Examples of GPDs measurements planned at 12 GeV. Projected data for the t-dependence of the transverse target spin asymmetry A_{UT} on the proton [23], shown for a single bin at $Q^2 = 2$ GeV^2 and x=0.25 (left) and for the beam-spin asymmetry A_{LU} on the neutron [24] for one bin in Q^2, x, t (right). The different lines indicate expected asymmetries for different values of the nucleon spin carried by u and d quarks as predicted by the VGG model.

while at the same time gather information on the fragmentation process thanks to the multi-dimensional analyses. Dedicated studies of higher twist distributions and spin orbit correlations in the target fragmentation region will be performed to control the validity of the underlying formalism in JLab kinematics. Special attention is given to the flavor decomposition of TMDs, thanks to the different nucleon targets and the excellent hadron identification in the final state achieved by time-of-flight and ring-imaging Cherenkov detection techniques.

Precise data from unpolarized liquid hydrogen and deuterium targets will be important to determine the role of the sea partons, for the study of the up-to-date poorly know transverse momentum dependence of the quark momentum distribution and for the study of the Boer-Mulders effect with pions [15] and kaons [16].

The goal of the experiments with longitudinally polarized NH_3 and ND_3 targets in conjunction with the high beam longitudinal polarization is the study of quark helicity with unprecedented precision, in particular at large x where powerful discrimination among models and potential implications for the quark angular momentum reside. The excellent particle ID will allow a full helicity flavor decomposition [17], in particular to constrain the contribution of the sea quarks. Moreover the setup will allow the study of azimuthal asymmetries originated by spin-orbit parton correlations by detecting pions [18] and kaons [19] in the final state.

The much anticipated use of the HD-ice, a novel type of target with only polarizable material except for a minimum amount of Aluminum for cooling, has the goal of minimizing the nuclear effects. Its use with transverse polarization is foreseen for precise extraction of the Sivers and transversity functions with flavor sensitivity in the SIDIS single-hadron [20] and double-hadron [21] production channels.

The exclusive program plans a comprehensive investigation of the DVCS process, with beam and target spin asymmetries on a longitudinally [22] and transversely polarized [23] proton target, and beam spin asymmetries on a neutron (deuteron) target [24]. Time-like Compton scattering and J/ψ photoproduction on proton target will also be studied [25]. Examples of the exclusive meson investigation are the disentanglement of the longitudinal and transverse components of the π^0 and η pseudo-scalar mesons electroproduction [26], to test the reaction models and eventually access the transversity GPDs, and the measurement of exclusive ϕ electroproduction [27], to access the gluon GPD and the nucleon gluonic radius at moderate x. In addition the measurement of the proton magnetic form factor at high Q^2 by detecting the electron quasi-elastic scattering off a deuteron target is planned [28].

7. Hall A and the precision frontier

The 12 GeV SIDIS two-stages program in Hall A is focused on high-statistics measurements of the neutron structure by using the world-leading polarized ^{3}He target. The first stage foresees the use of an upgraded version of the historical two-harm set-up. The apparatus is able to sustain very high luminosities, up to $10^{38} cm^{-2} s^{-1}$ but offer a limited acceptance. The second stage foresees the use of a barrel detector embedded in a large acceptance solenoid (SoLID) downstream of the target. Such a detector should be able to eventually conjugate high luminosity (up to $10^{36} cm^{-2} s^{-1}$) together with large acceptance, providing the ultimate precision limit in the multi-dimensional TMDs exploration at JLab, although with a limited flavor sensitivity because of the lack of kaon identification.

The use of the Super-Bigbite spectrometer (SBS) for detecting mesons and the BigBite (BB) spectrometer for detecting scattered electrons with a transversely-polarized ^{3}He target will allow to measure SIDIS reactions on both charged pions and charged kaons [29]. The spectrometers will be set at large angles in order to reach large-Q^2 and high x, while avoiding the excessive background at small angles. With the simultaneous neutral-pion channel data, isospin effects of SIDIS can be explored and models of the reaction-mechanism effects can be tested, important for high-precision studies of neutron transversity.

The SoLID detector was first proposed by the approved 12-GeV parity-violating DIS experiment [30] in conjunction with unpolarized targets and very high luminosity (up to $10^{39}\mathrm{cm}^{-2}\mathrm{s}^{-1}$). For the nucleon structure experiments, the detectors will be rearranged for forward angle (6.6-22 degrees) detection and charged-pion identification capability will be added. The very high statistical precisions in multi-dimension (x, z, p_T, Q^2) in conjunction with the open azimuthal angle acceptance anticipate a clean separation of the Fourier components of the cross-section while providing an excellent control of the systematic uncertainties.

The use of transversely polarized NH_3 and ^{3}He targets is planned to study the TMD distributions of proton [31] and neutron [32], respectively, and eventually disentangle the up and down quark distributions. The use of longitudinally polarized ^{3}He target [33], will allow measurements related to the longitudinal-transverse spin-orbit interference and the quark angular orbital angular momentum.

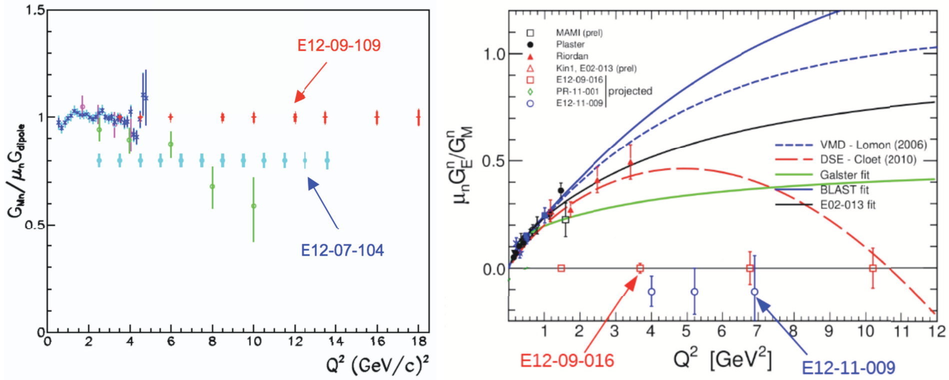

Fig. 4. Examples of nucleon form factor measurements planned at 12 GeV. Projections for the JLab measurements of the neutron form factors G_M^n (left) and G_E^n (right) with different techniques and apparatus (see text) in comparison to current available results and predictions.

The measurement of the nucleon form-factors of the neutron and proton at high-Q^2 will exploit different techniques using dedicated two-harm apparatus and the Hall-A BigHAND hadron calorimeter. The detection of double-spin asymmetries in polarized electron quasi-elastic scattering off a longitudinal-polarized ^{3}He target is used for the extraction of the neutron form factor G_E^n/G_M^n ratio [34]. The recoil polarization method is used for the study of the proton form factor G_E^n/G_M^n ratio [35]. A deuteron target is used to access the neutron magnetic form factor at high Q^2 by measuring the ratio of quasi-elastic scattering off neutron over proton [36]. A high-precision measurement of the helicity-independent and helicity-dependent DVCS cross-section is planned [37]. An experiment with the SoLID detector is planned to study the J/ψ production mechanism in the threshold region and to probe the color fields in the nucleon using the J/ψ color neutral object [38].

References

1. V. Barone, A. Drago and P.G. Ratcliffe, *Phys. Rep.* **359**, 1 (2002); V. Barone, F. Bradamante, A. Martin, *Prog. Part. Nucl. Phys.* **65**, 267 (2010).
2. A. Bacchetta *et al.*, *JHEP* **02**, 093 (2007); P.J. Mulders and R.D. Tangerman, *Nucl. Phys.* **B 461**, 197 (1996); erratumibid. **B 484**, 538 (1997).
3. D. W. Sivers, *Phys. Rev.* **D 41**, 83 (1990).
4. D. Boer and P. J. Mulders, *Phys. Rev.* **D 57**, 5780 (1998).
5. D. Müller et al., *Fortschritte der Physik*, **42**, 101 (1994); A. V. Radyushkin, *Phys. Lett.* **B 380**, 417 (1996); X. Ji, *Phys. Rev.* **D 55**, 7114 (1997).
6. X. Ji, *Phys. Rev. Lett.* **78**, 610 (1997).
7. M. K. Jones *et al.*, *Phys. Rev. Lett.* **84** (2000) 1398; O. Gayou *et al.*, *Phys. Rev.* **C 64** (2001) 038292; O. Gayou *et al.*, *Phys. Rev. Lett.* **88** (2002) 092301.
8. S. Stepanyan *et al.*, *Phys. Rev. Lett.* **87** 182002 (2001).
9. H. Mkrtchyan *et al.*, *Phys. Lett.* **B 665**, 20 (2008).
10. X. Qian *et al.*, *Phys.Rev.Lett.* **107** 072003 (2011); J. Huang *et al.*, *Phys.Rev.Lett.* **108** 052001 (2012).

11. JLab experiment E12-06-104, R. Ent *et al.*, (2006).
12. JLab experiment E12-09-017, R. Ent *et al.*, (2009).
13. JLab experiment E12-07-111, T. Horn *et al.*, (2007).
14. JLab experiment E12-09-011, T. Horn *et al.*, (2009).
15. JLab experiment E12-06-112, H. Avakian *et al.*, (2006).
16. JLab experiment E12-09-008, H. Avakian *et al.*, (2009).
17. JLab experiment E12-09-007, K. Hafidi *et al.*, (2009).
18. JLab experiment E12-07-107, P. Rossi *et al.*, (2007).
19. JLab experiment E12-09-009, H. Avakian *et al.*, (2009).
20. JLab experiment C12-11-111, M. Contalbrigo *et al.*, (2011).
21. JLab experiment C12-12-109, H. Avakian *et al.*, (2012).
22. JLab experiment E12-06-119, S. Sabatie *et al.*, (2006).
23. JLab experiment C12-10-010, L. Elouadrhiri *et al.*, (2010).
24. JLab experiment E12-11-003, S. Niccolai *et al.*, (2011).
25. JLab experiment E12-12-001, P. Nadel-Turonski *et al.*, (2012).
26. JLab experiment E12-06-108, V. Kubarovsky *et al.*, (2006).
27. JLab experiment E12-12-107, F.-X. Girod *et al.*, (2012).
28. JLab experiment E12-07-104, G. P. Gilfoyle *et al.*, (2007).
29. JLab experiment E12-09-018, B. Wojtsekhowski *et al.*, (2009).
30. JLab experiment E12-10-007, P. A. Souder *et al.*, (2010).
31. JLab experiment E12-10-006, H. Gao *et al.*, (2010).
32. JLab experiment E12-11-108, H. Gao *et al.*, (2011).
33. JLab experiment E12-11-007, J. Huang *et al.*, (2011).
34. JLab experiment E12-09-016, B. Wojstekhowski *et al.*, (2009).
35. JLab experiment E12-07-109, E. Brash *et al.*, (2007).
36. JLab experiment E12-09-019, B. Wojstekhowski *et al.*, (2009).
37. JLab experiment E12-06-114, C. M. Camacho *et al.*, (2006).
38. JLab experiment E12-12-006, Z.-E. Meziani *et al.*, (2012).